ELSEVIER

The influence of the ligand structure on activation of hafnocene polymerization catalysts: A theoretical study

Virve A. Karttunen [a], Mikko Linnolahti [a], Anniina Turunen [a], Tapani A. Pakkanen [a,*],
John R. Severn [b], Janne Maaranen [b], Esa Kokko [b], Päivi Pitkänen [b]

[a] *Department of Chemistry, University of Joensuu, P.O. Box 111, FI-80101 Joensuu, Finland*
[b] *Borealis Polymers Oy, R&D, P.O. Box 330, FIN-06101 Porvoo, Finland*

Abstract

The influence of ligand structure of hafnocenes on activation of the polymerization catalysts has been studied by quantum chemical methods. Altogether 54 hafnocenes were included in the analysis, supplemented by four zirconocenes for comparison. The trends in structural and electronic parameters relevant in the catalyst activation step were studied for the dichloride, dimethyl and cationic monomethyl forms of the catalysts. The effects of ligand modifications were analyzed as functions of the metal, ancillary cyclopentadienyl-based ligand, ligand substituent and the ligand bridge, making comparisons to experimental data. Generally, large aromatic ligands together with electron donating ligand substituents stabilize the catalytically active species, thus facilitating the catalyst activation process. The obtained trends are expected to aid in the development of new high-performance polymerization catalysts.
© 2007 Elsevier B.V. All rights reserved.

Keywords: Ab initio calculations; Metallocenes; Hafnium; Activation; Methylation

1. Introduction

Hafnocenes belong to Group IV metallocenes, which are frequently used as olefin polymerization catalysts. Metallocenes can produce highly uniform polymer structure with narrow molecular weight distributions. The polymerization activities are particularly high in the case of zirconocenes, which have been most widely studied by both experimental and theoretical methods. Generally, the analogous hafnocenes have lower polymerization activities, but have the benefit of producing higher molecular weight than the corresponding zirconocenes [1].

Prior to the initiation of the polymerization process, metallocene dichloride precursors need to be activated for generation of the catalytically active species. The activation is typically performed by methylaluminoxane (MAO) cocatalyst, exact structure, and hence mechanism of func-

tion, of which has remained unsolved [2]. The activation process starts with methylation of the metallocene precursor, which is followed by abstraction of either a methyl group from the dimethylated species or chlorine from the monomethylated species, to form the active cationic species (Scheme 1) [3]. The polymerization reaction itself takes place between the incoming monomers and the generated active metal center. The catalytic performance is sensitive for the conditions of polymerization, being influenced by factors such as temperature, solvent, monomer concentration and catalyst/co-catalyst ratio.

Alongside with the reaction conditions, the polymerization performance is strongly affected by the molecular structure of the metallocene catalyst. The ligand structure has a central role, correlations between the ligand structure and polymerization activity having been reported for zirconocenes [4]. The correlations have been interpreted to originate from differences in the accessibility of the active metal center, which is contributed by both steric and electronic effects [4]. Much less data is available for hafnocenes

---

Methylation
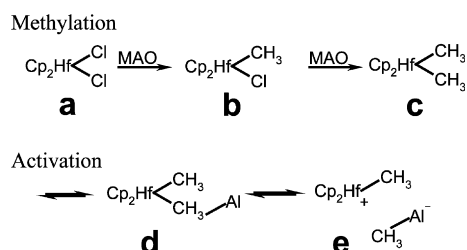
Activation

Scheme 1. Methylation and activation of a hafnocene dichloride with methylaluminoxane.

[1,5]. Nevertheless, the knowledge on zirconocenes provides useful guidelines for the performance of hafnocenes due to the similarity of the two metallocenes. From steric point of view, they are practically equal due to a similar ligand framework. Owing to the 4f lanthanide contraction of Hf, zirconocenes and hafnocenes are isostructural with practically same atomic radii [6]. Considering the dichloride precursor forms, the main structural difference between the two metallocenes is the M–Cl distance, which is about 0.02 Å shorter in hafnocenes [7]. Moreover, hafnium complexes usually possess stronger M–C bonds [8]. Hence, the bonds between the metal and the leaving groups (Cl, Me), i.e. the bonds which are broken during the activation step, are stronger in hafnocenes. Experimental measurements suggest methide abstraction from hafnocenes to be ca. 17 kJ/mol less exothermic than for zirconocenes. The stronger M–Cl and M–C bonds in hafnocenes have been interpreted to result in lower polymerization activity but higher molecular weight of the polymer in comparison to zirconocenes [2,9].

There are only a few previous quantum chemical studies on hafnocenes as polymerization catalysts [10,11]. The present theoretical study is motivated by the promise of the hafnocenes: they produce high molecular weight polymer but have room for improvement when it comes to polymerization activities. To screen potential ways of enhancing the activities of the hafnocenes, we study the influence of the ligand structure with focus on steric and electronic factors important in the catalyst activation step. Altogether 54 hafnocenes are included in the study, to analyze the effect of various ancillary ligands, ligand substituents and bridges between the ancillary ligands.

2. Computational methods

All metallocenes were fully optimized without any constraints. Hybrid density functional B3LYP [12–14] method with 6-31G∗ basis set was applied for all elements except Hf and Zr. For Hf, Los Alamos ECP [15] (LANL2DZ) was employed and for Zr the Huzinaga's all-electron extra basis (Zr, 433 321/433/421) [16]. The applied combinations of methods and basis sets have been previously shown to provide reliable structures for hafnocenes [17] and zirconocenes [18]. Optimizations were carried out with the Gaussian03 program package [19].

3. Results and discussion

3.1. Choice of the hafnocenes

The base for the studied set of hafnocenes is formed by experimentally characterized hafnocenes found from the Cambridge structural database. The hafnocenes were selected from the database with the following prerequisites: (a) exactly one Hf atom, (b) two cyclopentadienyl rings (c) two chlorines as leaving groups and (d) no other transition metals than Hf. Altogether 39 hafnocenes were included in the study. The crystallographically characterized hafnocenes (C1–C39 in Fig. 1) were supplemented with additional structures (H1–H15 in Fig. 1) to enable direct comparison of the influence of a greater variety of structural modifications. Conformational analysis was carried out for the hafnocenes H1–H15 to locate the global minimum conformations. The hafnocenes C1–C39 were studied in the conformation of the crystal structure.

3.2. Description of the steric and electronic effects

The ligand structures of the metallocenes give rise to various steric and electronic effects contributing to the feasibility of the activation step together with the subsequent polymerization steps. Several parameters measuring the steric and electronic environment of the hafnocenes were considered. The studied parameters were taken from a previous study, in which their influence is analyzed more deeply [4c].

The steric influence of the ligand framework is measured by three structural parameters: Hf–Cp′ distance, Cp′–Hf–Cp′ angle and Cp′–Cp′ plane angle (Cp′ = any cyclopentadienyl-based ligand). Generally, the accessibility of the metal center is improved by increasing the Hf–Cp′ distance, decreasing the Cp′–Hf–Cp′ angle and increasing the Cp′–Cp′ plane angle. It should be noted that the influence of the structural effect is actually less straightforward due to the simultaneous electronic effects they give rise to. This is best seen by considering the ring slippage angle (RSA), i.e. displacement of the ring centroid from the normal to the ring plane, which is defined by a combination of the Cp′–Hf–Cp′ angle and the Cp′–Cp′ plane angle (RSA = $1/2$(Cp′–Cp′ + Cp′–Hf–Cp′) −90). RSA affects the electron donating nature of the Cp′ ligand, changing the overlap between the metal and ligand orbitals [4c].

The electron donating nature of the Cp′ ligand significantly affects the relative stability of the active cationic species, thereby affecting the feasibility of the activation step and thus the concentration of the active species in the system. The stability of the active cationic form relative to the dichloride precursor (ΔE_x) can be calculated from

$$\Delta E_x = [E_e(L_x) - E_a(L_x)] - [E_e(L_0) - E_a(L_0)] \tag{1}$$

Here one ligand structure is selected as the reference (L_0) for the other ligand structures (L_x) to be compared with. E_e is the total energy of the cationic monomethyl form
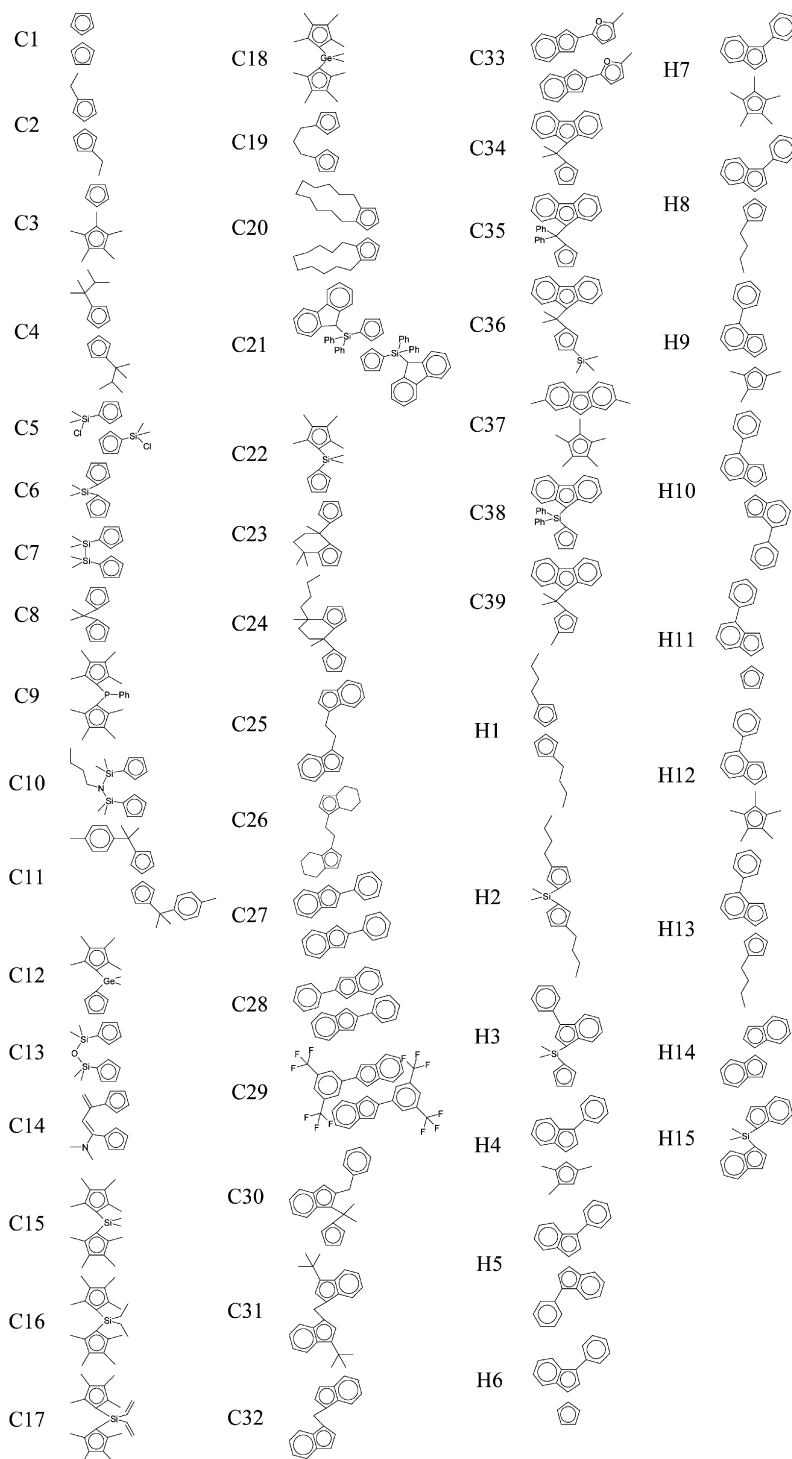
Fig. 1. Schematic ligand structures of the studied hafnocenes.

(**e** in Scheme 1) and E_a is the total energy of the dichloride precursor (a in Scheme 1). The relative stabilities of the dimethylated species can be calculated from Eq. (1) by changing E_e to E_c, which is the total energy of the dimethylated form (c in Scheme 1). The focus being on the ligand structures, the effects of cocatalysts are omitted throughout the paper.

Two metal–ligand bonds, Hf–Cl and Hf–CH$_3$, break in the activation process, and Hf–CH$_3^+$ at the beginning of the polymerization process. Since shorter bonds are usually stronger, these structural parameters provide information about the strengths of the relevant metal–ligand bonds.

The discussed parameters are listed in Table 1 for all studied hafnocenes. In the following, the effects of ligand

Table 1
Energies and geometries of hafnocene dichloride, dimethyl and monomethylated form

Structure	L₂MCl₂						L₂MMe₂							L₂MMe⁺						
	Hf–Cl (Å)	Hf–Cp (Å)[a]	Hf–Cp (Å)	Cp–Hf–Cp (°)	Cp–Cp (°)	RSA (°)	ΔE (kJ/mol)	Hf–C (Å)	Hf–Cp (Å)[a]	Hf–Cp (Å)	Cp–Hf–Cp (°)	Cp–Cp (°)	RSA (°)	ΔE (kJ/mol)	Hf–C (Å)	Hf–Cp (Å)[a]	Hf–Cp (Å)	Cp–Hf–Cp (°)	Cp–Cp (°)	RSA (°)
C1	2.427	2.238		129.5	52.7	1.1	0	2.259	2.262		133.2	49.2	1.2	0	2.210	2.189		138.7	40.7	−0.3
C2	2.435	2.243		130.4	56.1	3.3	17	2.259	2.279		131.5	54.9	3.2	−25	2.232	2.192	2.184	137.1	44.3	0.7
C3	2.435	2.247		131.3	51.0	1.1	9	2.263	2.272	2.274	134.0	48.8	1.4	−30	2.226	2.174	2.198	138.3	41.7	0.0
C4	2.434	2.255		129.3	54.1	1.7	7	2.263	2.282		131.1	50.8	1.0	−57	2.235	2.186	2.197	137.4	43.7	0.5
C5	2.421	2.245		129.3	53.0	1.2	−2	2.259	2.276		131.4	50.7	1.0	−104	2.237	2.222	2.209	135.5	43.7	−0.4
C6	2.421	2.241		125.2	60.3	2.8	8	2.252	2.266		125.1	59.5	2.3	−1	2.211	2.178		128.2	56.2	2.2
C7	2.430	2.239		130.9	51.3	1.1	3	2.261	2.264		133.4	48.9	1.2	−24	2.216	2.185		139.7	39.9	−0.2
C8	2.414	2.220		116.2	71.4	3.8	16	2.250	2.246		115.7	71.1	3.4	16	2.208	2.169		118.4	68.1	3.2
C9	2.424	2.251		125.5	64.8	5.1	26	2.255	2.277		125.0	64.0	4.5	−22	2.227	2.174		128.3	58.9	3.6
C10	2.434	2.234		131.6	50.6	1.1	4	2.267	2.260		134.5	47.9	1.2	−32	2.213	2.173		138.7	43.3	1.0
C11	2.434	2.256		129.1	54.0	1.6	7	2.262	2.284		131.7	50.1	0.9	−63	2.239	2.203		129.6	43.3	−3.6
C12	2.427	2.252	2.247	126.8	59.9	3.4	18	2.257	2.276	2.272	126.5	59.0	2.7	−21	2.220	2.188	2.169	129.9	54.6	2.3
C13	2.415	2.207	2.239	129.1	54.1	1.6	4	2.263	2.268		134.6	47.2	0.9	−106	2.245	2.211		139.6	40.2	−0.1
C14	2.427	2.224	2.237	127.7	53.5	0.6	5	2.258	2.260	2.246	128.8	52.3	0.6	−19	2.215	2.177	2.162	132.8	47.6	0.2
C15	2.433	2.258		128.1	61.6	4.8	26	2.255	2.289		127.6	60.8	4.2	−31	2.230	2.177	2.180	131.1	54.9	3.0
C16	2.429	2.266		128.3	62.1	5.2	27	2.255	2.290		127.8	60.8	4.3	−32	2.230	2.176		131.3	54.6	2.9
C17	2.429	2.263		128.1	61.8	5.0	26	2.258	2.286		127.5	60.7	4.1	−33	2.230	2.178		131.1	55.0	3.0
C18	2.433	2.261		128.6	60.1	4.4	27	2.256	2.289		128.1	59.2	3.7	−35	2.230	2.179		131.7	53.3	2.5
C19	2.432	2.234		129.8	50.0	−0.1	4	2.264	2.254		131.7	49.3	0.5	−17	2.212	2.180		137.5	40.5	−1.0
C20	2.427	2.237	2.251	130.6	56.2	3.4	11	2.268	2.269		133.9	52.1	3.0	−39	2.222	2.183		139.4	43.8	1.6
C21	2.427	2.247	2.243	129.4	53.6	1.5	8	2.259	2.278	2.275	131.6	50.9	1.3	−123	2.238	2.214	2.211	132.6	49.4	1.0
C22	2.426	2.251	2.246	126.2	61.6	3.9	18	2.254	2.275		125.8	60.8	3.3	−16	2.220	2.168	2.186	129.2	56.3	2.7
C23	2.416	2.224	2.236	116.1	72.0	4.0	17	2.253	2.250	2.263	115.6	72.5	4.1	0	2.213	2.167	2.174	118.4	68.7	3.5
C24	2.415	2.238	2.224	116.1	72.0	4.1	17	2.253	2.262	2.248	115.7	72.3	4.0	−3	2.214	2.174	2.167	118.5	68.6	3.6
C25	2.407	2.280		125.6	62.4	4.0	−4	2.244	2.294		125.1	61.2	3.1	−49	2.237	2.204	2.180	128.5	52.0	0.2
C26	2.431	2.249		125.2	61.2	3.2	24	2.257	2.276		125.1	60.5	2.8	−28	2.223	2.168	2.178	128.9	54.2	1.6
C27	2.407	2.286		130.9	54.1	2.5	−14	2.244	2.309		134.0	49.5	1.7	−94	2.232	2.199	2.166	139.1	40.3	−0.3
C28	2.408	2.290		131.3	56.5	3.9	−16	2.242	2.307		132.5	47.7	0.1	−102	2.234	2.171	2.178	139.3	38.7	−1.0
C29	2.399	2.287	2.279	131.1	50.1	0.6	−13	2.246	2.310	2.307	132.6	47.4	0.0	−55	2.238	2.171	2.175	140.7	37.7	−0.8
C30	2.401	2.263	2.211	117.5	72.8	5.1	13	2.248	2.287	2.236	116.8	72.4	4.6	−27	2.225	2.173	2.166	119.7	68.1	3.9
C31	2.401	2.290		118.1	78.1	8.1	14	2.233	2.326		116.7	78.0	7.4	−38	2.222	2.197	2.182	121.7	70.0	5.9
C32	2.395	2.262		116.9	73.3	5.1	3	2.234	2.286		115.9	72.7	4.3	−21	2.215	2.151	2.175	120.7	66.8	3.7
C33	2.408	2.287		131.0	54.2	2.6	−9	2.244	2.311		132.5	51.4	1.9	−106	2.233	2.233	2.219	137.5	43.9	0.7
C34	2.401	2.329	2.192	118.2	74.9	6.6	7	2.241	2.346	2.215	117.7	74.1	5.9	−31	2.236	2.225	2.155	120.6	69.7	5.1
C35	2.402	2.317	2.187	117.5	75.4	6.4	7	2.242	2.334	2.209	117.0	74.5	5.7	−44	2.225	2.192	2.147	120.5	69.5	5.0
C36	2.404	2.340	2.196	118.4	76.0	7.2	11	2.239	2.360	2.227	117.5	75.5	6.5	−51	2.227	2.214	2.135	120.6	68.3	4.5
C37	2.408	2.501	2.228	134.9	62.6	8.7	9	2.240	2.551	2.258	137.5	61.5	9.5	−75	2.231	2.210	2.188	141.5	42.1	1.8
C38	2.402	2.395	2.216	128.5	66.8	7.7	−2	2.239	2.421	2.238	128.4	66.2	7.3	−59	2.246	2.281	2.176	128.8	55.8	2.3
C39	2.403	2.327	2.195	118.6	75.4	7.0	11	2.240	2.349	2.221	118.0	74.8	6.4	−35	2.224	2.225	2.152	120.9	70.1	5.5
H1	2.436	2.237		131.3	52.5	1.9	8	2.261	2.266		133.7	51.8	2.8	−21	2.223	2.183	2.179	138.1	42.5	0.3
H2	2.421	2.247		126.2	61.8	4.0	15	2.255	2.272		125.9	61.4	3.7	−20	2.216	2.177	2.173	129.3	56.6	2.9
H3	2.408	2.309	2.230	126.8	63.6	5.2	3	2.243	2.337	2.253	126.4	63.1	4.8	−40	2.225	2.201	2.178	129.1	57.9	3.5
H4	2.433	2.287	2.238	132.3	45.3	−1.2	6	2.259	2.331	2.264	134.0	43.7	−1.2	−64	2.236	2.244	2.198	136.2	39.0	−2.4

H5	2.415	2.280	2.230	128.5	59.5	4.0	−1	2.242	2.310	2.252	132.3	55.0	3.6	−81	2.224	2.210	2.215	136.6	49.6	3.1
H6	2.425	2.271	2.240	129.1	49.3	−0.8	2	2.257	2.306	2.269	131.8	46.8	−0.7	−43	2.269	2.239	2.199	137.3	36.4	−3.2
H7	2.424	2.326	2.240	130.8	55.5	3.1	13	2.252	2.360	2.256	133.8	51.8	2.8	−79	2.233	2.224	2.198	136.8	46.8	1.8
H8	2.428	2.274	2.228	129.5	49.9	−0.3	6	2.259	2.311	2.259	132.2	47.6	−0.1	−46	2.264	2.242	2.203	137.0	38.4	−2.3
H9	2.414	2.290	2.232	129.4	57.4	3.4	3	2.261	2.312		131.5	54.6	3.0	−55	2.228	2.191	2.170	136.9	44.4	0.6
H10	2.415	2.274		131.2	47.4	−0.7	−7	2.247	2.299	2.255	133.6	45.2	−0.6	−72	2.228	2.175	2.174	140.1	37.7	−1.1
H11	2.420	2.266	2.229	129.7	49.1	−0.6	0	2.261	2.297	2.270	132.4	46.3	−0.7	−46	2.267	2.206	2.202	137.1	38.5	−2.2
H12	2.416	2.297	2.241	131.0	55.3	3.1	6	2.261	2.321	2.260	134.0	52.7	3.4	−60	2.220	2.199	2.177	137.4	44.5	1.0
H13	2.411	2.284	2.230	129.5	57.4	3.4	0	2.260	2.308		133.4	54.1	3.8	−49	2.222	2.188	2.174	137.1	44.8	1.0
H14		2.288		130.4	58.0	4.2	−16	2.246	2.299		133.8	55.7	4.7	−67	2.215	2.177	2.196	139.0	42.8	0.9
H15	2.399			126.8	63.8	5.3	−3	2.237	2.310		126.3	62.7	4.5	−47	2.226	2.192	2.177	130.3	55.7	3.0

a Upper Cp′ in schematic ligand structure in Fig. 1.

modifications are analyzed in detail for each parameter. For calculation of the relative energies, C1 (see Fig. 1) is set as the reference. In unsymmetrical hafnocenes, the two Hf–Cl and Hf–CH₃ distances may have different values. Whenever this is the case, the shorter Hf–Cl and the longer Hf–CH₃ distances are included in the comparisons, because two Hf–Cl bonds are broken from the dichloride precursor and one Hf–C from the dimethyl form. The range of the parameters are listed in Table 2.

3.3. The effect of metal

Selection of the metal affects both polymerization activity and molecular weight of the polymer. The experimental data available for zirconocenes will be utilized below in the analysis of hafnocenes. Structural parameters of four analogous hafnocenes and zirconocenes are compared in Table 3 in dichloride, dimethyl and cationic monomoethyl forms. In the dichloride form the structural parameters, excluding the M–Cl distance, are practically equal. The M–Cl distance is 0.023–0.030 Å shorter in hafnocenes, which is about the same as observed experimentally.[7] The same trends apply for the dimethylated form, M–C distances being 0.13–0.18 Å shorter in hafnocenes. More differences are seen in the cationic monomethyl form. For hafnocenes, M–C distance is shorter by 0.011–0.019 Å, the M–Cp′ shorter by 0.007–0.023 Å and the Cp′–Cp′ plane angle smaller by 0.5–7.0°. As noted in previous literature, the apparent reason for the lower activity of hafnocenes in comparison to zirconocenes is the stronger bonds between the metal and the leaving groups [8]. The smaller Cp′–Cp′ angles in hafnocene cations increase steric hindrance, thereby decreasing the accessibility of the active reaction centers. This may contribute to the lower activity of hafnocenes.

Table 2
The ranges of energetic and structural parameters of the hafnocenes

	Maximum	Minimum
Relative stability of L₂HfMe⁺ (kJ/mol)[a]	−123	16
Relative stability of L₂HfMe₂(kJ/mol)[a]	−16	27
Hf–Cp′ (Å)	Cl₂: 2.501	Cl₂: 2.187
	Me₂: 2.551	Me₂: 2.209
	Me⁺: 2.281	Me⁺: 2.135
Cp′–Hf–Cp′ (°)	Cl₂: 135	Cl₂: 116
	Me₂: 138	Me₂: 116
	Me⁺: 141	Me⁺: 118
Cp′–Cp′ (°)	Cl₂: 78	Cl₂: 45
	Me₂: 78	Me₂: 44
	Me⁺: 70	Me⁺: 36
RSA (°)	Cl₂: 8.7	Cl₂: −1.2
	Me₂: 9.5	Me₂: −1.1
	Me⁺: 5.9	Me⁺: −3.6
Hf–Cl (Å)	2.436	2.395
Hf–CH₃(Å)	2.268	2.233
Hf-CH₃⁺(Å)	2.269	2.208

a Negative values indicate higher relative stability.

Table 3
Comparison of geometry parameters of analogous hafnocenes and zirconocenes

Structure	Metal	L2MCl2						L2MMe2						L2MMe+					
		Hf–Cl (Å)	Hf–Cp (Å)[a]	Hf–Cp (Å)	Cp–Hf–Cp (°)	Cp–Cp (°)	RSA (°)	Hf–C (Å)	Hf–Cp (Å)[a]	Hf–Cp (Å)	Cp–Hf–Cp (°)	Cp–Cp (°)	RSA (°)	Hf–C (Å)	Hf–Cp (Å)[a]	Hf–Cp (Å)	Cp–Hf–Cp (°)	Cp–Cp (°)	RSA (°)
C1	Hf	2.427	2.238		129.5	52.7	1.1	2.259	2.262		133.2	49.2	1.2	2.210	2.189		138.7	40.7	-0.3
	Zr	2.450	2.241		130.1	53.3	1.7	2.273	2.266		134.4	48.7	1.5	2.228	2.200		135.5	47.6	1.5
C8	Hf	2.414	2.220		116.2	71.4	3.8	2.250	2.246		115.7	71.1	3.4	2.208	2.169		118.4	68.1	3.2
	Zr	2.444	2.224		116.7	72.4	4.6	2.268	2.252		116.5	72.3	4.4	2.227	2.186		118.4	71.0	4.7
C6	Hf	2.421	2.241		125.2	60.3	2.8	2.252	2.266		125.1	59.5	2.3	2.211	2.178		128.2	56.2	2.2
	Zr	2.444	2.244		125.7	61.3	3.5	2.269	2.269		125.9	61.3	3.6	2.229	2.201		127.9	60.6	4.3
H6	Hf	2.425	2.271	2.230	129.1	49.3	-0.8	2.257	2.306	2.252	131.8	46.8	-0.7	2.269	2.239	2.199	137.3	36.4	-3.2
	Zr	2.449	2.272	2.235	130.1	49.5	-0.2	2.270	2.312	2.259	134.1	45.8	-0.1	2.281	2.246	2.206	138.0	36.9	-2.6

[a] Upper Cp′ in schematic ligand structure in Fig. 1.

3.4. The effect of Cp′ ligand

The studied hafnocenes contain either cyclopentadienyl (Cp), indenyl (Ind), tetrahydroindenyl (Thind) or fluorenyl (Flu) as Cp′ ligands. The differences between Cp and Ind can be seen by comparing C1 with H14 and C6 with H15 (see Fig. 1). By changing from Cp to Ind, the relative stability of the cationic monomethyl form increases by 46–67 kJ/mol, the relative stability of the dimethylated from increasing by 11–16 kJ/mol. The Hf–Cp′ distances get longer and the Cp′–Hf–Cp angles and the Cp′–Cp′ plane angle generally larger, thus also increasing the ring slippage angle. The Hf–Cl and Hf–CH3 distances become somewhat shorter whereas the Hf–CH3+ distances are slightly elongated.

The differences between Cp and CpFlu can be seen by comparing C8 with C34. CpFlu increases the relative stability of the cationic monomethyl form by 47 kJ/mol and that of the dimethyl form by 8 kJ/mol. The Hf–Cp′ distances to Flu increase, and to Cp, decrease. Cp′–Hf–Cp angles, Cp′–Cp′ plane angles and RSAs increase. The Hf–C bond of the cationic methyl form becomes shortened by about 0.03 Å.

The differences between Ind and Thind can be seen by comparing C25 with C26. Thind decreases the relative stabilities of both the cationic monomethyl and the dimethyl forms by 21 and 28 kJ/mol, respectively. The Hf–Cp bonds become shortened, while the bond angles are only slightly affected. The Hf–Cl and Hf–CH3 bonds become longer, whereas Hf–CH3+ bond of the cationic form becomes shorter.

The limited number of reported experimental polymerization studies of hafnocenes carried out at identical conditions [5], complicates the comparison between the experiments and the theoretical work. More abundant data is available for zirconocenes, polymerization behaviour of which may provide useful guidelines. Considering ethene polymerization by zirconocenes, the polymerization activities typically increase in the order Cp < Thind < Ind [1,5d,5g]. This follows the order of the relative stabilities of the cationic forms, suggesting increased polymerization activity because of larger concentration of active reaction centers in the polymerization system.

3.5. The effect of ligand substituent

The influences of methyl substituents can be figured out by comparing C1 to C3, C6 to C22 and C15, C12 to C18, H6 to H4 and H7, and H11 to H9 and H12. The methyl substituents improve the relative stability of the cationic monomethyl from, the stability further improving as a function of the number of methyl substituents. On the other hand, the methyl groups likewise destabilize the dimethyl form. The Hf–Cp distances become longer for the dichloride and dimethyl forms, whereas the cationic monomethyl remains practically unaffected. In average, the methyl groups slightly increase the Cp–Hf–Cp angles,

Cp′–Cp planes angles and RSAs. The trends are not apparent, however. Neither are they for the leaving groups. It is notable however, that the Hf–CH$_3^+$ bond distances of the non-methylated, benzyl-substituted CpInd hafnocenes (H6 and H11) are particularly long. The influences of larger alkyl substituents can be figured out by comparing C1 to C2, C4, C20 and H1, C32 to C31, C34 to C39, H6 to H8 and H11 to H13. Their effects are very similar to those of the methyl substituents.

Next we study the influence of aromatic substituents, the effects of which can be seen by comparing C1 to C11 and C21 and H14 to C27, C28, H5, H10 and C33. Aromatic substituents strongly stabilize the cationic monomethyl form, while slightly destabilizing the dimethyl form. In most cases, the effects on structural parameters are marginal. However, the Hf–CH$_3^+$ distances are elongated, in average by 0.02 Å. The influence of the position of phenyl substituents on indenyl ring can be seen by comparing C28 to H5 and H10, H6 to H11, H4 to H9, H7 to H12, and H8 to H13. The relative stabilities of the cationic monomethyl forms generally increase in the order 4-phenyl < 3-phenyl < 2-phenyl, while the relative stabilities of the dimethyl forms increase in the order 3-phenyl < 4-phenyl < 2-phenyl. The major structural effects of the position of the substituent are longer Hf–CH$_3^+$ distances for 1-phenyl than for 2- and 4-phenyl, and nonsystematic changes in Cp′–Hf–Cp′ angles, Cp′–Cp′ plane angles and RSAs. As most extreme examples, the change from 3-benzyl in H5 to 4-benzyl in H10 decreases the Cp′–Cp′ plane angle by 12°, whereas the change from 3-benzyl in H4 to 4-benzyl in H9 increases the Cp′–Cp′ plane angle by 12°.

C1 and C5, together with C28 and C29, form the pairs for studying the influences of electron withdrawing substituents. The chlorine of C5 binds to hafnium in the cationic monomethyl form. This results in a high relative stability of the cation but is unlikely to increase the concentration of active center accessible by the monomers due to blocking the active reaction center. The typical of electron withdrawing substituents can be seen in C28 versus C29 comparison, the fluorines destabilizing the active species. The dimethylated form becomes destabilized, as well. The only major structural changes are the decreases in Cp′–Cp′ plane angles and RSAs in the dichloride form.

Experimental polymerization studies on zirconocenes have shown that the electron withdrawing substituents generally result in decreased polymerization activities, whereas enhanced polymerization activities are attainable by the use of electron donating substituents. [1,5d] This correlates with the relative stability of the active species. In this particular case, the data includes a set of hafnocenes, namely H3, H4, H7, H11 and H12, for which polymerization studies have been performed under the same conditions. [5r] The polymerization activities increase in the order H11 < H3 < H12 < H4 < H7. Addition of methyl substituents thus results in enhanced activity (compare H4 versus H7 and H11 versus H12) as well as changing the phenyl substituent from position 3 to position 4 (H7 versus H12). It is notable that the activity order is in a agreement with the relative stabilities of the active species, which increase in the order H3 < H11 < H12 < H4 < H7.

3.6. The effect of bridge

The influences of bridges can figured out by comparing (a) C1 to C6, C7, C8, C10, C13, C14, C19, C23 and C24, (b) H14 to H15, C25 and C32, (c) H1 to H2, and (d) H6 to H3. Variation in the bridges is large, this study containing the most common bridges [5q] together with a few less common ones. The changes in the relative stabilities of the cationic monomethyl forms are less pronounced than in the case other ligand modifications. The one significant exception is C13, cationic form of which is strongly stabilized by coordination of the bridge oxygen to the hafnium center. Generally, the one-carbon bridges decrease the relative stability of the cation, whereas many-atom bridges increase the stability. The dimethyl forms are systematically destabilized due to introduction of bridges, the variation between the different bridges being less significant.

The bridges have major influences on the structural parameters, however, and in particular to the angular parameters. Typically, introduction of a bridge decreases the Cp′–Hf–Cp′ angles and increases the Cp′–Cp angles, both by a same magnitude, thus leaving the RSA practically unaffected. The effect is clearly the strongest for one-atom bridges, and stronger for carbon than for silicon. The changes in Hf–Cl, Hf–CH$_3$ and Hf–CH$_3^+$ bond lengths are mostly small with no apparent trends.

Concerning experimental polymerization studies on zirconocenes, the addition of Si(CH$_3$)$_2$ increases the activity, producing higher activities than the corresponding carbon bridge [5q]. Comparing C(CH$_3$)$_2$ and Si(CH$_3$)$_2$ bridges, the carbon bridge opens the Cp–Cp plane angle by about 10° more than the corresponding silicon bridge. At the same time, the Cp–M–Cp angle is about 10 degrees larger for the Si-bridged metallocene. While large Cp–Cp plane angle opens the reaction site for the monomer, it also opens it for the counterion. Furthermore, the larger Cp–M–Cp angle of the Si-bridged metallocene shields the metal center and thereby increases the metal-counterion separation. As a consequence, the beneficial effect of the Si(CH$_3$)$_2$ bridge could be related to the weaker interaction between the metal and the counterion.

3.7. Summary of ligand effects

The main effects of ligand modifications to the studied parameters are summarized in Table 4. The relative stability of the active species is mostly stabilized by large aromatic Cp′ ligand and electron donating substituents, and destabilized by electron withdrawing substituents and short bridges. Large aromatic Cp′ ligands stabilize the dimethyl form, as well, whereas the electron donating substituents destabilize it. The destabilization of the dimethyl form is the strongest in the case of short bridges. The Hf–Cp′ bond

Table 4
Summary of the effects of ligand modifications of hafnocenes on the studied parameters

	Typically increased by:	Typically decreased by:	Highest	Lowest
Rel. stability of L_2HfMe^+	Large aromatic Cp′ ligands, electron donating substituents	Electron withdrawing substituents, short bridges	C21	C8
Rel. stability of L_2HfMe_2	Large aromatic Cp′ ligands	Short bridges	H14	C18
Hf–Cp′	Large aromatic Cp′ ligands	Short bridges	C37 (Cl_2, Me_2); C38 (Me^+)	C35 (Cl_2, Me_2); C36 (Me^+)
Cp′–Hf–Cp′	Large aromatic Cp′ ligands	Short bridges	C37	C23 (Cl_2, Me_2); C8 (Me^+)
Cp′–Cp′	Short bridges	Long bridges	C31 (Cl_2, Me_2); C39 (Me^+)	H4 (Cl_2, Me_2); H6 (Me^+)
RSA	Large aromatic Cp′ ligands	Benzyl-substituents	C37 (Cl_2, Me_2); C31 (Me^+)	H4 (Cl_2, Me_2); H11 (Me^+)
Hf–Cl	Alkyl-substituted Cp	Large aromatic Cp′ ligands	H1	C32
Hf–CH_3	Alkyl-substituted Cp	Large aromatic Cp′ ligands	C20	C31
Hf–CH_3^+	Large aromatic Cp′ ligands	Plain Cp	H6	C8

distances and Cp′–Hf–Cp′ angles seem to linked to each other, both being increased by large aromatic Cp′ ligands and decreased by short bridges. The Cp′–Cp′ plane angles are most dependent on the bridge, increasing with short, and decreasing with large bridges. Simultaneously increasing both Cp′–Hf–Cp′ angles and Cp′–Cp′ plane angles, the large aromatic Cp′ ligands produce the largest ring slippage angles. The effect is particularly strong in the case of fluorenyl ligands. Surprisingly, the benzyl-substituents systematically decrease the RSA.

The Hf–Cl and Hf–CH_3 distances usually follow the same trends, the longest distances being obtained by the alkyl-substituted Cp ligands. The large aromatic Cp′ ligands shorten the Hf–Cl and Hf–CH_3 distances, being at shortest in the case of indenyl. The Hf–CH_3^+ distances appear to be linked to the relative stabilities of the cations typically increasing with large aromatic Cp′ ligands.

4. Conclusions

The steric and electronic effects of the ligand framework of hafnocene polymerization catalysts were analyzed for a dataset of 54 complexes. The dichloride, dimethyl and cationic monomethyl forms of the catalysts were optimized by hybrid density functional B3LYP method. Several structural and energetic parameters were examined as a function of the ligand structure of the hafnocenes, including comparisons made to zirconocenes.

The hafnocenes possess shorter M–Cl and M–CH_3 distances than the corresponding zirconocenes, apparently contributing to the lower polymerization activities but higher molecular weight of the polymer produced by hafnocenes. Generally, large aromatic Cp′ ligands together with electron donating and aromatic substituents increase the relative stability of the active cationic species due to donation of electrons to the electron-deficient metal. The consequently increased concentration of active metal centers in the polymerization system should result in enhanced polymerization activities, as previously shown for zirconocenes. On the other hand, electron withdrawing substituents destabilize the active species. The structural parameters, having both steric and electronic effects, are mostly influenced by large aromatic Cp′ ligands and the bridge structure between the Cp′ ligands. Overall, the obtained trends in ligand modifications may turn out useful in the development of new hafnocenes, combining high polymerization activities with high molecular weight of the polymer.

References

[1] H.G. Alt, A. Köppl, Chem. Rev. 100 (2000) 1205.
[2] E.Y.-X. Chen, T.J. Marks, Chem. Rev. 100 (2000) 1391.
[3] (a) W. Kaminsky, R. Steiger, Polyhedron 7 (1988) 2375;
(b) D. Cam, U. Giannini, Makromol. Chem. 193 (1992) 1049.
[4] (a) K. Hortmann, H.-H. Brintzinger, New J. Chem. 16 (1992) 51;
(b) C. Janiak, K.C.H. Lange, U. Versteeg, D. Lentz, P.H.M. Budzelaar, Chem. Ber. 129 (1996) 1517;
(c) M. Linnolahti, T.A. Pakkanen, Macromolecules 33 (2000) 9205;
(d) P.C. Möhring, N.J. Coville, Coord. Chem. Rev. 250 (2006) 18.
[5] (a) E. Giannetti, G.M. Nicoletti, R.J. Mazzocchi, Polym. Sci., Polym. Chem. Ed. 23 (1985) 2117;
(b) D.T. Mallin, M.D. Rausch, J.C.W. Chien, Polym. Bull. 20 (1988) 421;
(c) J. Tian, B. Huang, Macromol. Rapid Commun. 15 (1994) 923;
(d) P.C. Moehring, N.J.J. Coville, Organomet. Chem. 479 (1994) 1;
(e) G.M. Diamond, A.N. Chernega, P. Mountford, M.L.H. Green, J. Chem. Soc., Dalton Trans. Inorg. Chem. 6 (1996) 921;
(f) W. Kaminsky, Macromol. Chem. Phys. 197 (1996) 3907;
(g) N.M. Bravaya, Z.M. Dzhabieva, V.P. Maryin, V.V. Strelets, Polymery 42 (1997) 591;
(h) H.G. Alt, M. Jung, J. Organomet. Chem. 580 (1999) 1;
(i) A. Yano, M. Sone, S. Yamada, S. Hasegawa, A. Akimoto, Macromol. Chem. Phys. 200 (1999) 924;
(j) A. Yano, M. Sone, S. Yamada, S. Hasegawa, M. Sato, A. Akimoto, J. Mol. Catal. A-Chem. 156 (2000) 133;
(k) D.E.B. Lopes, M.L. Dias, M.F.V. Marques, A.V. Grofov, Polym. Bull. 45 (2000) 365;
(l) G. Tian, B. Wang, X. Dai, S. Xu, X. Zhou, J. Sun, J. Organomet. Chem. 634 (2001) 145;
(m) S. Xu, X. Deng, B. Wang, X. Zhou, L. Yang, Y. Li, Y. Hu, F. Zou, Y. Li, Macromol. Rapid Commun. 22 (2001) 708;
(n) B. Wang, B. Mu, X. Deng, H. Cui, S. Xu, X. Zhou, F. Zou, Y. Li, L. Yang, Y. Li, Y. Hu, Chem-Eur. J. 11 (2005) 669;
(o) A.V. Grafov, C.L. Firme, I.A. Grafova, F. Benetollo, M.L. Dias, M.J.M. Abadie, Polymer 46 (2005) 9626;

(p) A.V. Grafov, D.E.B. Lopes, I.A. Grafova, M.L. Dias, M.F.V. Marques, J. Mol. Catal. A-Chem. 229 (2005) 59;

(q) B. Wang, Coord. Chem. Rev. 250 (2006) 242;

(r) T. Piel, T. Saarinen, B. Lofgren, E. Kokko, J. Maaranen, P. Pitkanen, Macromol. Chem. Phys. 208 (2007) 851.

[6] F.A. Cotton, G. Wilkinson, Advanced Inorganic Chemistry, 3rd ed., Wiley Interscience, New York, 1972, p. 927.

[7] R.M. Shaltout, J.Y. Corey, N.P. Rath, J. Organomet. Chem. 503 (1995) 205.

[8] (a) M.F. Lappert, D.S. Patil, J.B. Pedley, J.C.S. Chem. Comm. 20 (1975) 830;

(b) L.E. Schock, T.J. Marks, J. Am. Chem. Soc. 110 (1988) 7701;

(c) J.A. Martinho Simoes, J.L. Beauchamp, Chem. Rev. 90 (1990) 629;

(d) W.A. King, S. Di Bella, A. Gulino, G. Lanza, I.L. Fragala, C.L. Stern, T.J. Marks, J. Am. Chem. Soc. 121 (1999) 355.

[9] P.A. Deck, C.L. Beswick, T.J. Marks, J. Am. Chem. Soc. 120 (1998) 1772.

[10] See for example: (a) P. Margl, L. Deng, T. Ziegler, Top. Catal. 7 (1999) 187;

(b) E. Zurek, T. Ziegler, Faraday Discuss 124 (2003) 93;

(c) K. Vanka, Z. Xu, M. Seth, T. Ziegler, Top Catal. 34 (2005) 143.

[11] I. Silanes, J.M. Mercero, J.M. Ugalde, Organometallics 25 (2006) 4483.

[12] A.D. Becke, J. Chem. Phys. 98 (1993) 5648.

[13] C. Lee, W. Yang, R.G. Parr, Phys. Rev. B 37 (1988) 785.

[14] P.J. Stephens, F.J. Devlin, C.F. Chabalowski, M.J. Frisch, J. Phys. Chem. 98 (1994) 11623.

[15] P.J. Hay, W.R. Wadt, J. Chem. Phys. 82 (1985) 270.

[16] S. Huzinaga, Gaussian Basis Sets for Molecular Calculations, Elsevier, Amsterdam, 1984.

[17] V.A. Karttunen, M. Linnolahti, T.A. Pakkanen, J. Maaranen, P. Pitkänen, Theor. Chem. Acc., DOI: 10.1007/s00214-007-0375-6.

[18] M. Linnolahti, P. Hirva, T.A. Pakkanen, J. Comput. Chem. 22 (2001) 51.

[19] M.J. Frisch, G.W. Trucks, H.B. Schlegel, G.E. Scuseria, M.A. Robb, J.R. Cheeseman, J.A. Montgomery Jr., T. Vreven, K.N. Kudin, J.C. Burant, J.M. Millam, S.S. Iyengar, J. Tomasi, V. Barone, B. Mennucci, M. Cossi, G. Scalmani, N. Rega, G.A. Petersson, H. Nakatsuji, M. Hada, M. Ehara, K. Toyota, R. Fukuda, J. Hasegawa, M. Ishida, T. Nakajima, Y. Honda, O. Kitao, H. Nakai, M. Klene, X. Li, J.E. Knox, H.P. Hratchian, J.B. Cross, V. Bakken, C. Adamo, J. Jaramillo, R. Gomperts, R.E. Stratmann, O. Yazyev, A.J. Austin, R. Cammi, C. Pomelli, J.W. Ochterski, P.Y. Ayala, K. Morokuma, G.A. Voth, P. Salvador, J.J. Dannenberg, V.G. Zakrzewski, S. Dapprich, A.D. Daniels, M.C. Strain, O. Farkas, D.K. Malick, A.D. Rabuck, K. Raghavachari, J.B. Foresman, J.V. Ortiz, Q. Cui, A.G. Baboul, S. Clifford, J. Cioslowski, B.B. Stefanov, G. Liu, A. Liashenko, P. Piskorz, I. Komaromi, R.L. Martin, D.J. Fox, T. Keith, M.A. Al-Laham, C.Y. Peng, A. Nanayakkara, M. Challacombe, P.M.W. Gill, B. Johnson, W. Chen, M.W. Wong, C. Gonzalez, J.A. Pople, GAUSSIAN 03, Revision C.02, Gaussian Inc., Wallingford, CT, 2004.